

AD-A188 999

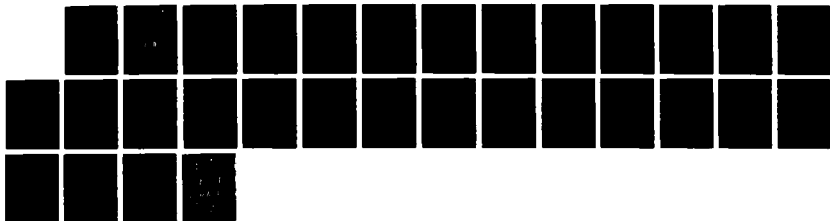
WAVE PROPAGATION IN LAMINATED COMPOSITE PLATES(U)
COLORADO UNIV AT BOULDER DEPT OF MECHANICAL ENGINEERING
S K DATTA ET AL. AUG 87 CUMER-87-4 N00014-86-K-0200

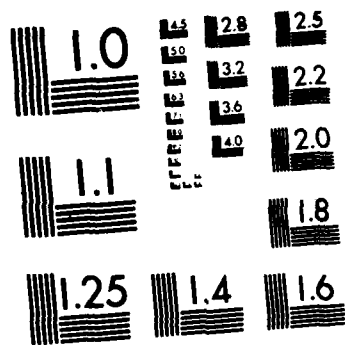
1/1

UNCLASSIFIED

FFG 11/4

ML





MICROCOPY RESOLUTION TEST CHART
NATIONAL BUREAU OF STANDARDS-1963-A

② M

DTIC FILE COPY

Contract N00014-86-K-0280

WAVE PROPAGATION IN LAMINATED COMPOSITE PLATES

S.K. Datta
University of Colorado, CIRES

A.H. Shah
University of Manitoba

R.L. Bratton, Research Assistant and
T. Chakraborty, Research Associate
University of Colorado, CIRES

CUMER 87-4

August, 1987

AD-A188 999

DTIC
ELECTE
DEC 3 1 1987
S D
GD

DISTRIBUTION STATEMENT A
Approved for public release
Distribution Unlimited

WAVE PROPAGATION IN LAMINATED COMPOSITE PLATES

S.K. Datta, Department of Mechanical Engineering and CIRES
University of Colorado, Boulder

A.H. Shah, Department of Civil Engineering
University of Manitoba, Winnipeg

R.L. Bratton, Research Assistant
and

T. Chakraborty, Research Associate
Department of Mechanical Engineering and CIRES
University of Colorado, Boulder

↙ A stiffness method has been used in this paper to study dispersive wave propagation in a laminated anisotropic plate. The advantage of this method is in its usefulness in obtaining numerical results for the dispersion characteristics of waves propagating in a plate with an arbitrary number of arbitrarily anisotropic laminae. We have applied this method here, as a way of illustration, to a plate made up of transversely isotropic laminae with the axis of isotropy of each lamina lying in the plane of the lamina. Results thus obtained are shown to agree well with the exact solutions for isotropic and transversely isotropic single layered plates. We present numerical results for cross-ply $(0^\circ/90^\circ/0^\circ)$ laminated composite plates and show that the frequency spectrum in this case differ considerably from that for a single layered (0°) plate.

(submitted for publication in the Journal of the Acoustical Society of America)

Introduction

In the past dynamic behavior of infinite periodically laminated medium has been studied extensively. A review of the literature on exact and approximate analysis of this problem can be found in [1,2]. In [2] a stiffness method was presented for studying harmonic wave propagation in a periodically laminated infinite medium. In this method each lamina is divided into several sublayers and the displacement distribution through the thickness of each sublayer is approximated by polynomial interpolation functions. These functions involve number of discrete generalized coordinates, which are the displacements and tractions at the interfaces between the adjoining sublayers. This ensures continuity of these quantities at these interfaces. By applying Hamilton's principle the dispersion equation is obtained as a standard algebraic eigenvalue problem. Eigenvalues and eigenvectors of this equation yield the frequencies of propagating and evanescent modes and the associated displacements and tractions at the interfaces. Results obtained by this method for an infinite medium with isotropic laminae were shown to agree well with exact solutions [1].

In this paper we use a similar technique to study dispersion of waves in a laminated plate. Although the method is easily applied to arbitrarily anisotropic laminae, we have illustrated the method for the case when each lamina is transversely isotropic with the symmetry axis lying parallel to the lamina. This study is motivated by the desire to model wave propagation in a continuous fiber-reinforced laminated plate. If it is assumed that the wave lengths are much longer than the fiber diameters and spacing, then each lamina can be modeled as a homogeneous transversely isotropic medium with the symmetry axis parallel to the fibers. The overall effective elastic properties of such a medium can be calculated from the fiber and matrix properties by using an effective modulus theory [3,4]. Such an assumption has been made in this paper. Thus this study examines the dispersion characteristics of guided waves in a layered anisotropic plate.

Although wave propagation in a homogeneous isotropic plate has been thoroughly studied using exact or approximate means by Mindlin [5] and many others, not many exact solutions for layered plates have been reported. Most of the works on layered



or	
31	<input checked="" type="checkbox"/>
ed	<input type="checkbox"/>
	<input type="checkbox"/>
<i>per the</i>	
ility Codes	
and/or	
Special	

A-1

plates have used approximate plate theories or effective modulus theory for the entire plate (Dong and Nelson [6] for discussion) because of the extreme complexities involved in the equations obtained when the exact three dimensional linear theory of elasticity is used. For a two layer or three layer (sandwich) isotropic plate the governing dispersion equation becomes tractable and has been discussed in [7-9].

Wave propagation in a monoclinic crystal plate has been fully investigated in [10-12]. However, to our knowledge, no exact solutions for laminated anisotropic plate are available. In [6,13,15] the authors present a stiffness method to study this problem. They use interpolation functions for the displacements that involve as generalized coordinates the displacements at the interfaces between layers and at the middle of the layers. Although the technique yields generally good results for the frequency spectrum, it does not lead directly to the determination of the tractions at the interfaces.

For studying scattering by cracks or inhomogeneities using a hybrid method in which the localized region near the scatterers is represented by finite elements and the exterior solution by superposition of modes (propagating and non-propagating) it is necessary not only to get accurate approximations to displacements, but also to the tractions at the boundary separating the inner and outer regions (for applications of this hybrid technique see [15-17]). It is with this application in mind that we present in this paper a stiffness method that incorporates as generalized coordinates displacements and tractions at the interfaces between the layers (and sublayers). As mentioned before the results obtained by this method for a periodically laminated infinite medium agree well with known exact solutions. Here we show that for an isotropic and transversely isotropic plate the method yields results in excellent agreement with the exact solutions. It is noted that the present method using the same number of sublayers yields more accurate results at high frequencies than obtained by the technique of Dong et al [6,13,14]. Intuitively it is clear that as the number of sublayers tend to infinity the results based on the present formulation, where the continuity of displacement and traction is maintained at the interfaces, should approach the exact continuum solution.

Governing Equations

We consider time harmonic waves in a plate composed of n laminae. For simplicity in analysis it will be assumed that each lamina is transversely isotropic with the symmetry axis aligned with either the x or the y axis (Fig. 1). This assumption is not necessary for the development of the equations but, it is made here to keep the algebra as simple as possible for the anisotropic problem at hand. Under this assumption the wave propagation problem reduces to two uncoupled ones: plane strain in which the displacement components are u_x , u_z , and SH or antiplane strain when the only nonzero displacement component is u_y . So in the following we shall treat these two separately.

Plane Strain

Consider the i th lamina bounded by $z = z_{i-1}$ and $z = z_{i+1}$. The stress strain relation in this lamina will be given by

$$\begin{Bmatrix} \sigma_{xx} \\ \sigma_{zz} \\ \sigma_{xz} \end{Bmatrix} = \begin{bmatrix} c_{11}^{(i)} & c_{13}^{(i)} & 0 \\ c_{13}^{(i)} & c_{33}^{(i)} & 0 \\ 0 & 0 & c_{55}^{(i)} \end{bmatrix} \begin{Bmatrix} \epsilon_{xx} \\ \epsilon_{zz} \\ \gamma_{xz} \end{Bmatrix} \quad (1)$$

where σ_{ij} and ϵ_{ij} are the stress and strain components, respectively, and we have written $\gamma_{xz} = 2\epsilon_{xz}$. Note that if the y axis is the axis of symmetry, then

$$c_{11}^{(i)} = c_{33}^{(i)} \quad \text{and} \quad c_{55}^{(i)} = \frac{1}{2} \left(c_{11}^{(i)} - c_{13}^{(i)} \right)$$

Then the problem is equivalent to that of an isotropic one. In order to get good numerical results each lamina will be divided into several sublayers, m , say. Within the i th sublayer we will choose a local coordinate with the origin at the mid-plane and x_j, y_j, z_j , parallel to the global x, y, z axes,

respectively. Let $2h_j$ be the thickness of this sublayer. Denoting $u^{(j)}$ to be the displacement at a point in the j th lamina we write

$$u_x^{(j)} = u_{j-1} f_1 + u_j f_2 + \left[\frac{1}{c_{55}^{(j)}} x_j \frac{\partial}{\partial x_j} - \frac{\partial w_{j-1}}{\partial x_j} \right] f_3 + \left[\frac{1}{c_{55}^{(j)}} y_j \frac{\partial}{\partial x_j} - \frac{\partial w_j}{\partial x_j} \right] f_4 \quad (2)$$

$$u_z^{(j)} = w_{j-1} f_1 + w_j f_2 + \left[\frac{1}{c_{33}^{(j)}} \sigma_{j-1} - \frac{c_{13}^{(j)}}{c_{33}^{(j)}} \frac{\partial w_{j-1}}{\partial x_j} \right] f_3 + \left[\frac{1}{c_{33}^{(j)}} \sigma_j - \frac{c_{13}^{(j)}}{c_{33}^{(j)}} \frac{\partial w_j}{\partial x_j} \right] f_4$$

where f_n ($n=1, \dots, 4$) are cubic polynomials in the local coordinate z_j given by

$$f_1 = \frac{1}{4} (2-3\eta_j + \eta_j^2), \quad f_2 = \frac{1}{4} (2+3\eta_j - \eta_j^2)$$

$$f_3 = \frac{h_j}{4} (1-\eta_j - \eta_j^2 + \eta_j^3), \quad f_4 = \frac{h_j}{4} (-1 - \eta_j + \eta_j^2 + \eta_j^3)$$

Here $\eta_j = z_j/h_j$ and u_j, w_j, x_j, σ_j are the values of u_x, u_z, σ_{xz} , and σ_{zz} at the j th node. These nodal values of the displacement and traction components are functions of $x_j (=x)$ and t . In this paper it will be assumed that the time dependence is of the form $e^{-i\omega t}$, ω being the circular frequency. The factor $e^{-i\omega t}$ will be dropped in the sequel.

The equations governing the nodal generalized coordinates $\{u_j, \bar{x}_j, w_j, \sigma_j\}$ will be obtained using Hamilton's principle. For this purpose we calculate the lagrangian, L , per unit length in the y -direction of the plate as

$$\begin{aligned}
 L &= \sum_{i=1}^n L^{(i)} = \sum_{i=1}^n \sum_{j=1}^{m_i} \frac{1}{2} \int \left\{ \int_{-h_j}^{h_j} \rho^{(j)} \left\{ \begin{matrix} \dot{u} \\ \dot{w} \end{matrix} \right\}^T \left\{ \begin{matrix} \dot{u} \\ \dot{w} \end{matrix} \right\} dz_j - \int_{-h_j}^{h_j} \left\{ \begin{matrix} h_j \\ -h_j \end{matrix} \right\}^T [c^{(j)}] \{\epsilon\} dz_j \right\} dx \\
 &= \sum_{i=1}^n \sum_{j=1}^{m_i} L^{(i)}_j \tag{4}
 \end{aligned}$$

The overbar denotes complex conjugate.

Using (2) in the strain-displacement relation, and in turn in (4), we get the expression for $L^{(i)}_j$ as

$$L^{(i)}_j = \frac{1}{2} \int \left[\frac{\omega^2}{\rho} \left\{ \bar{q} \right\}^T [C_2] \left\{ q \right\} + \left\{ \bar{q} \right\}^T [C_1] \{q\} + \left\{ \bar{q} \right\}^T [C_3] \{q'\} + \left\{ \bar{q} \right\}^T [M] \{q\} \right]$$

$$- \left\{ \bar{q} \right\}^T [e_1] \{q''\} - \left\{ \bar{q} \right\}^T [e_2] \{q'\} -$$

$$\left\{ \bar{q} \right\}^T [e_3] \{q''\} - \left\{ \bar{q} \right\}^T [e_4] \{q\} -$$

$$\left\{ \bar{q} \right\}^T [e_5] \{q''\} - \left\{ \bar{q} \right\}^T [e_6] \{q'\} -$$

$$\left\{ \begin{matrix} - \\ q \end{matrix} \right\}^T [e_s] (q) - \left\{ \begin{matrix} - \\ q \end{matrix} \right\}^T [e_s] (q') - \left\{ \begin{matrix} - \\ q \end{matrix} \right\}^T [e_s] (q) dx \quad (5)$$

where $\{q\}$ is defined as

$$\{q\} = \left\{ u_{j-1}, x_{j-1}^{\gamma_{j-1}}, w_{j-1}, \sigma_{j-1}, u_j, x_j^{\gamma_j}, w_j, \sigma_j \right\}^T \quad (6)$$

and the primes denote derivatives with respect to x . The matrices $[C_2]$, $[C_3]$, etc. are defined in the Appendix I.

The Lagrangian for the complete plate is obtained by summing over all the layers and its variation leads to the governing equation for the plate as

$$\begin{aligned} & \omega^2 (-[C_2] [Q''] - [C_1] [Q'] + [M] [Q]) \\ & - ([E_1] [Q^{IV}] + [E_2] [Q'''] + [E_3] [Q''] + \\ & [E_4] [Q'] + [E_5] [Q]) = 0 \end{aligned} \quad (7)$$

Note that the matrices $[C_1]$, $[M]$, $[E_1]$, $[E_2]$, and $[E_4]$ are symmetric, whereas, the others are skew-symmetric. These assembled matrices are defined in Appendix I. It is seen that the generalized coordinate vector $\{Q\}$ satisfies a fourth order homogeneous ordinary differential equation in x .

A solution to equation (7) can be assumed in the form

$$\{Q\} = [Q_0] e^{ikx} \quad (8)$$

where $[Q_0]$ represents the amplitude vector. Substituting (8) in (7) we get a set of linear homogeneous equations to solve for $[Q_0]$:

$$k^4[K_1] - ik^3[K_2] - k^2[K_3] + ik[K_4] + [K_5] [Q_0] = 0 \quad (9)$$

where

$$[K_1] = [E_1]$$

$$[K_2] = [E_2]$$

$$[K_3] = [E_3] + \omega^2[C_2]$$

$$[K_4] = [E_4] + \omega^2[C_1]$$

$$[K_5] = [E_5] - \omega^2[M]$$

For nontrivial solution the determinant of the coefficient matrix must be zero. This equation is the dispersion equation to solve for the eigenvalues k for given ω . Alternatively, Eq. (9) can also be written as $([K_\rho] - \omega^2[M_\rho]) [Q_0] = 0$

where

$$[K_\rho] = k^4[K_1] - ik^3[K_2] - k^2[E_3] + ik[E_4] + [E_5], [M_\rho] = [M] - ik[C_1] + k^2[C_2]$$

This leads to the eigenvalue problem for solving ω^2 for given k .

Antiplane Strain

The derivation given above is for the case of plane strain. The antiplane strain case can be considered in a similar manner and that results in a much simpler frequency/wave number equation. In this case we assume

$$u_y^{(j)} = v_{j-1} f_1 + v_j f_2 + \frac{1}{c_{55}^{(j)}} \tau_{j-1} f_3 + \frac{1}{c_{55}^{(j)}} \tau_j f_4 \quad (11)$$

$$\text{Here } \tau = c_{44}^{(j)} \partial u_y^{(j)} / \partial z.$$

The corresponding eigenvalue problem for the wave number is

$$(-k^2[K_6] + [K_8]) \{Q_0\} = 0 \quad (12)$$

and that for the frequency is

$$([K_5] - \omega^2[M_5]) \{Q_0\} = 0 \quad (13)$$

where

$$[K_5] = k^2[K_6] + [K_7]$$

$$[K_8] = \omega^2 [M_5] - [K_7]$$

and the corresponding matrices for the sublayer from which these are assembled are def-

ined in Appendix I. The vector $\{q\}$ is defined as $\{v_{j-1}, \tau_{j-1}, v_j, \tau_j\}^T$

As illustrative examples we show equations (9) and (10) for an isotropic plate, a fiber-reinforced (0°) homogeneous plate, a three-layered ($0^\circ/90^\circ/0^\circ$) plate and a four-layered ($0^\circ/90^\circ/0^\circ/90^\circ$) plate. These results are discussed in the next section. We also present some numerical results for the SH case.

Numerical Results and Discussion

In order to validate the method we first considered an isotropic plate with Poisson's ratio, $\nu = 0.31$. A full discussion of the frequency spectrum for this case was given by Mindlin [5]. Both the eigenvalue problems (9) and (10) were solved. The comparison of the results obtained for real and imaginary wave numbers with those of Ref. [5] are shown in Fig. 2. In this figure $\Omega = \frac{\omega H}{\pi\sqrt{\mu/\rho}}$, $\gamma = \frac{kH}{\pi}$, where H is thickness of the

plate. For this computation the plate was divided into 25 sublayers. It is seen that the results agree with the exact solution extremely well at low and moderate frequencies. The agreement at high frequencies is also quite reasonable. We also used the interpolation functions adopted by Dong and Huang [15], and obtained the frequency spectrum keeping the same number of sublayers. Comparison of the results with the exact solution is shown in Fig. 3. The loss of accuracy at high frequencies is evident. Of course, the accuracy will improve if more sublayers are taken [6].

We then considered a fiber-reinforced plate when the fibers are aligned along the x-axis (0°). The properties of the plate are given in Table 1. As mentioned before, for propagation in the 0° (90°) direction the problem is tractable analytically. The frequency equation for this case is given in Appendix II. Figure 4 shows the comparison of the frequency spectrum obtained by the present method with the exact solution for propagation

in the x-direction. It is seen that the comparison is excellent. In this figure

$$\Omega = \frac{\omega H}{2\pi \sqrt{(C_{55}/\rho)_{0^\circ}}} \text{ and } \gamma = \frac{kH}{2\pi}. \text{ It is seen that as } k \rightarrow \infty \text{ the slopes of the disper-}$$

sion curves for the first symmetric and antisymmetric modes tend to the ratio $V_R/\sqrt{C_{55}/\rho}$, where V_R is the Rayleigh wave velocity in the x-direction. For the discretization method we used 15 sublayers.

The next problem considered was a sandwich plate with $0^\circ/90^\circ/0^\circ$ configuration. Figure 5 shows the dispersion curves. These curves differ considerably from those shown in Fig. 4. It is seen that the cut-off frequencies are lowered as well as the slopes of the curves. Branches of imaginary wave numbers are also quite different. In these computations we used 15 sublayers also.

To see the comparison between our results and those obtained by the author of Ref. [14] we considered a 4-layer ($0^\circ/90^\circ/0^\circ/90^\circ$) plate with the properties* given in [14]. Solid lines in Fig. 6 are Dong and Huang's results using 20 sublayers. Open circles and dashed lines are ours using the same number of sublayers. The agreement deteriorates at high frequencies. For the same composite plate we show in Fig. 7 the complex frequency branches. Solid dots are obtained by the method of [14].

Finally, figures 8 and 9 show the SH wave spectra for homogeneous (0°) and three-layer ($0^\circ/90^\circ/0^\circ$) plates. Although the curves look very similar, it is interesting to note that the cut-off frequencies are increased in the latter case. This is contrary to what was found in the plane strain case.

* $(C_{11})_{0^\circ} = 21.289 \times 10^6 \text{ psi}$; $(C_{11})_{90^\circ} = 0.592 \times 10^6 \text{ psi}$; $(C_{33})_{0^\circ} = 2.3186 \times 10^6 \text{ psi}$; $(C_{33})_{90^\circ}$

$= 0.850 \times 10^6 \text{ psi}$; $\rho = 1 \frac{\text{g}}{\text{cm}^3}$

Conclusion

A stiffness method using through-thickness interpolation functions for the displacements that maintain continuity of displacements and tractions at the interfaces between the layers has been used to study guided waves in a laminated composite plate. It is shown that the results agree with exact known solutions for homogeneous plates and also with their numerical solutions. The advantage of the method is that it is more accurate at high frequencies with smaller number of sublayers than others in which only displacement continuity is enforced. Also, tractions and displacements are obtained as eigenvectors, so that the former need not be calculated by differentiation afterwards.

Numerical results presented show significant differences between the dispersion curves for the homogeneous fiber-reinforced plate and the cross-ply laminated plate.

Although the case of wave propagation along a principal direction has been studied, the method is easily applicable to off-axis propagation. For purposes of illustration only a small number of laminae has been considered. But, because we divide each lamina into several sublayers, each of these sublayers can have different properties. So any number of laminae can be considered.

Acknowledgement

The work reported has been supported by a grant from the Office of Naval Research (#N00014-86-K-0280; Program Manager: Dr. Y. Rajapakse) and grants (MSM-8609813 and INT-8521422) from the National Science Foundation. Partial support was also received from the Natural Science and Engineering Research Council of Canada (A-7988).

The first author gratefully acknowledges the hospitality provided by the University College, Galway, where part of this work was done, and where he had many helpful discussions with Dr. P.M. O'Leary. He is grateful also to the University of Colorado for the award of a Faculty Fellowship for the academic year 1986-1987.

Table 1. Properties of 0° and 90° laminae. All the stiffnesses are in units of 10^{11} N/m².

	ρ (g/cm ³)	C_{11}	C_{22}	C_{12}	C_{44}	C_{55}
0° lamina	1.2	1.6073	0.1392	0.0644	0.0350	0.0707
90° lamina	1.2	0.1392	1.6073	0.0644	0.0707	0.0350

References

1. J.D. Achenbach, Generalized continuum theories for directionally reinforced solids. Archiv. Mech. 28, 257 (1976)
2. A. H. Shah and S. K. Datta, Harmonic waves in a periodically laminated medium. Int. J. Solids Str. 18, 397 (1982)
3. Z. Hashin and B. W. Rosen, The elastic moduli of fiber-reinforced materials. J. Appl. Mech. 31, 223 (1964).
4. S. K. Datta, H. M. Ledbetter, and R. D. Kriz, Calculated elastic constants of composites containing anisotropic fibers. Inst. J. Solids Str., 20, 429 (1984).
5. R. D. Mindlin, Waves and vibrations in isotropic elastic plates. Proc. 1st Symp. Naval Str. Mech. Pergamon Press, 199 (1960).
6. S. B. Dong and R. B. Nelson, On natural vibrations and waves in laminated orthotropic plates, J. Appl. Mech., 39, 739 (1972)
7. Y. Y. Yu, Forced flexural vibrations of elastic sandwich plate. J. Appl. Mech. 27, 535 (1960).
8. J. P. Jones, Wave propagation in two-layered medium. J. Appl. Mech. 31, 213 (1964).
9. P. C. Y. Lee and N. Chang, Harmonic waves in elastic sandwich plates. J. Elasticity 9, 52 (1979)
10. E. G. Newman and R. D. Mindlin, Vibrations of monoclinic crystal plate. J. Acoust. Soc. Am. 29, 1206 (1957)
11. R. K. Kaul and R. D. Mindlin, Vibrations of an infinite, monoclinic crystal plate at high frequencies and long wavelengths. J. Acoust. Soc. Am. 34, 1985 (1962).
12. R. K. Kaul and R. D. Mindlin, Frequency spectrum of a monoclinic crystal plate. J. Acoust. Soc. Am. 34, 1902 (1962).
13. S. B. Dong and K. E. Pauley, Plane waves in anisotropic plates. J. Eng. Mech. Div. ASCE. 104, 802 (1978).
14. S. B. Dong and K. H. Hwang, Edge vibrations in laminated composite plates. J. Appl. Mech. 52, 433 (1985)
15. M. Koshiha, H. Morita, and M. Suzuki, Finite-element analysis of discontinuity problem of SH modes in an elastic plate waveguide. Electron. Lett. 17, 480 (1981)
16. Abduljakbar, S. K. Datta, and A. H. Shah, Diffraction of horizontally polarized shear waves by normal edge cracks in a plate. J. Appl. Phys. 52, 461, (1983)
17. M. Koshiha, S. Karakida, and M. Suzuki, Finite-element analysis of Lamb wave scattering in an elastic plate waveguide. IEEE Trans. Sonics Ultrasonics. SU-31, 18 (1984)

Appendix I

We first define the following matrices:

$$[N_1] = \begin{bmatrix} 0 & 0 & -f_1 & 0 & 0 & 0 & -f_2 & 0 \\ -C_{12}/C_{33}f_1 & 0 & 0 & 0 & -C_{12}/C_{33}f_2 & 0 & 0 & 0 \end{bmatrix}$$

$$[N_2] = \begin{bmatrix} f_1 & 1/C_{33}f_1 & 0 & 0 & f_2 & 1/C_{33}f_2 & 0 & 0 \\ 0 & 0 & f_1 & 1/C_{33}f_1 & 0 & 0 & f_2 & 1/C_{33}f_2 \end{bmatrix}$$

$$[d] = \begin{bmatrix} 0 & 0 & -f_1 & 0 & 0 & 0 & f_2 & 0 \\ 0 & 0 & 0 & 0 & 0 & 0 & 0 & 0 \\ -C_{12}/C_{33}f_1 & 0 & 0 & 0 & -C_{12}/C_{33}f_2 & 0 & 0 & 0 \end{bmatrix}$$

$$[b] = \begin{bmatrix} f_1 & 1/C_{33}f_1 & 0 & 0 & f_2 & 1/C_{33}f_2 & 0 & 0 \\ -C_{12}/C_{33}f_1 & 0 & 0 & 0 & -C_{12}/C_{33}f_2 & 0 & 0 & 0 \\ 0 & 0 & f_1-f_2 & 1/C_{33}f_1 & 0 & 0 & f_2-f_1 & 1/C_{33}f_2 \end{bmatrix}$$

$$[a] = \begin{bmatrix} 0 & 0 & 0 & 0 & 0 & 0 & 0 & 0 \\ 0 & 0 & f_1 & 1/C_{33}f_1 & 0 & 0 & f_2 & 1/C_{33}f_2 \\ f_1 & 1/C_{33}f_1 & 0 & 0 & f_2 & 1/C_{33}f_2 & 0 & 0 \end{bmatrix}$$

Then $[C_1]$, $[C_2]$, etc. can be written as

$$[C_1] = \int_{-h(j)}^{h(i)} \rho^j [N_1]^T [N_1] dz$$

$$[C_2] = \int \rho^{(j)} [N_1]^T [N_2] dz$$

$$[M] = \int \rho^{(j)} [N_2]^T [N_2] dz$$

$$[e_1] = \int [d]^T [C^{(j)}] [d] dz$$

$$[e_2] = \int [d]^T [C^{(j)}] [b] dz$$

$$[e_3] = \int [d]^T [C^{(j)}] [a] dz$$

$$[e_4] = \int [b]^T [C^{(j)}] [b] dz$$

$$[e_5] = \int [b]^T [C^{(j)}] [a] dz$$

$$[e_6] = \int [a]^T [C^{(j)}] [a] dz$$

For antiplane motion we define:

$$[N] = \left[f_1, \frac{1}{C^{(j)}} f_2, f_3, \frac{1}{C^{(j)}} f_4 \right]$$

Then we get

$$[m] = \int \rho^{(j)} [N]^T [N] dz$$

$$[k_1] = \int C_{33}^{(j)} [N]^T [N] dz$$

$$[k_2] = \int C_{33}^{(j)} [N^*]^T [N^*] dz$$

$$[C_1] = U(C_1 - C_1^T)$$

$$[C_2] = UC_2, [M] = Um, [E_1] = Ue_1$$

$$[E_2] = U(e_2 - e_2^T), E_3 = U(e_3 + e_3)$$

$$[E_4] = U(e_4^T - e_4), [E_5] = Ue_5$$

$$[K_1] = UK_1, [K_2] = UK_2, [M_3] = UM_3$$

Appendix II

For the propagation of waves along the plate of transversely isotropic material considered here the dispersion equation separates into two, one for the symmetric motion and the other for the antisymmetric case. In the former case we get

$$\frac{\tan(s_1 H/2)}{\tan(s_2 H/2)} = \frac{s_1 E_1 T_2}{s_2 E_2 T_1} \quad (II.1)$$

whereas, for the latter we have

$$\frac{\tan(s_1 H/2)}{\tan(s_2 H/2)} = \frac{s_2 E_2 T_1}{s_1 E_1 T_2} \quad (II.2)$$

In writing (II.1) and (II.2) we have defined the following quantities,

$$\begin{aligned} \alpha &= C_{11}/C_{33}, & \beta &= C_{33}/C_{55} \\ E_1 &= \beta(k_2^2 - s_1^2) + k^2(\delta^2 - \delta - \alpha\beta) \\ E_2 &= \beta(k_2^2 - s_2^2) + k^2(\delta^2 - \delta - \alpha\beta) \\ T_1 &= k_2^2 - k^2\alpha + s_1^2(\delta - 1) \\ T_2 &= k_2^2 - k^2\alpha + s_2^2(\delta - 1) \\ \delta &= 1 + C_{13}/C_{33}, & k_2^2 &= \omega^2/(C^{55}/\rho) \end{aligned}$$

$$s_{1,2} = \frac{1}{2\beta} [-(k^2\gamma - k_2^2(1+\beta)) \pm \{(k^2\gamma - k_2^2(1+\beta))^2 -$$

$$4\beta(k_2^2 - k^2)(k_2^2 - k^2\alpha)\}^{\frac{1}{2}}]$$

$$\gamma = 1 + \alpha\beta - \delta^2$$

List of Figures

1. Geometry of the laminated plate.
2. Comparison of the exact dispersion curves with numerical results for an isotropic plate. Poisson's ratio is 0.31.
3. Comparison of the results obtained by the method of Ref. [15] with the exact results.
4. Comparison of the results obtained by the present method for a fiber-reinforced plate with the exact results.
5. Dispersion curves for a laminated ($0^\circ/90^\circ/0^\circ$) plate.
6. Comparison of the dispersion curves for a $0^\circ/90^\circ/0^\circ/90^\circ$ plate obtained by the present method with those obtained using the technique of Ref. [14].
7. Complex frequency branches for a $0^\circ/90^\circ/0^\circ/90^\circ$ plate. - present method, - method of Ref. [14].
8. Dispersion curves for SH waves in a fiber-reinforced plate.
9. Dispersion curves for SH waves in a laminated ($0^\circ/90^\circ/0^\circ$) plate.

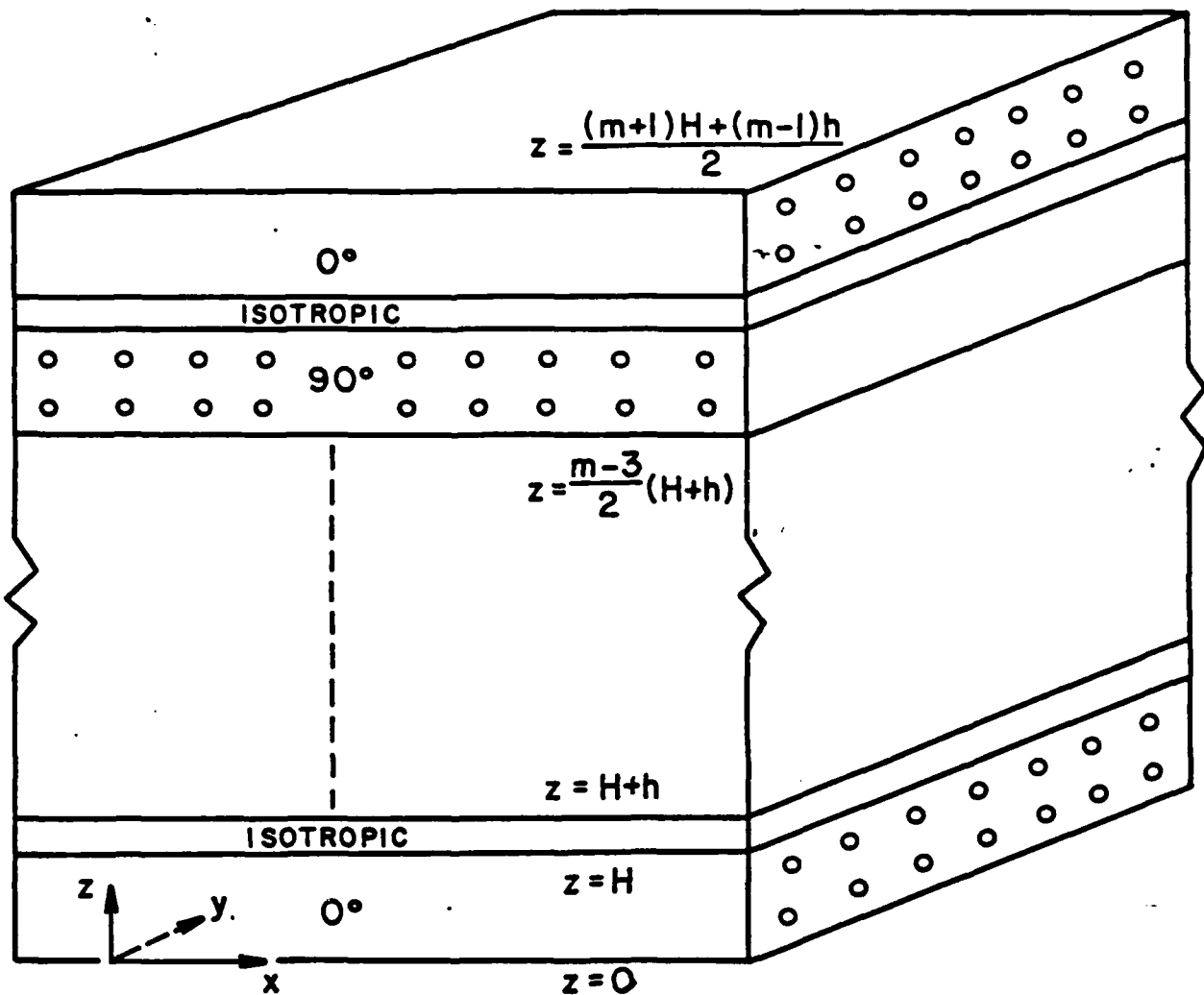


Fig. 1

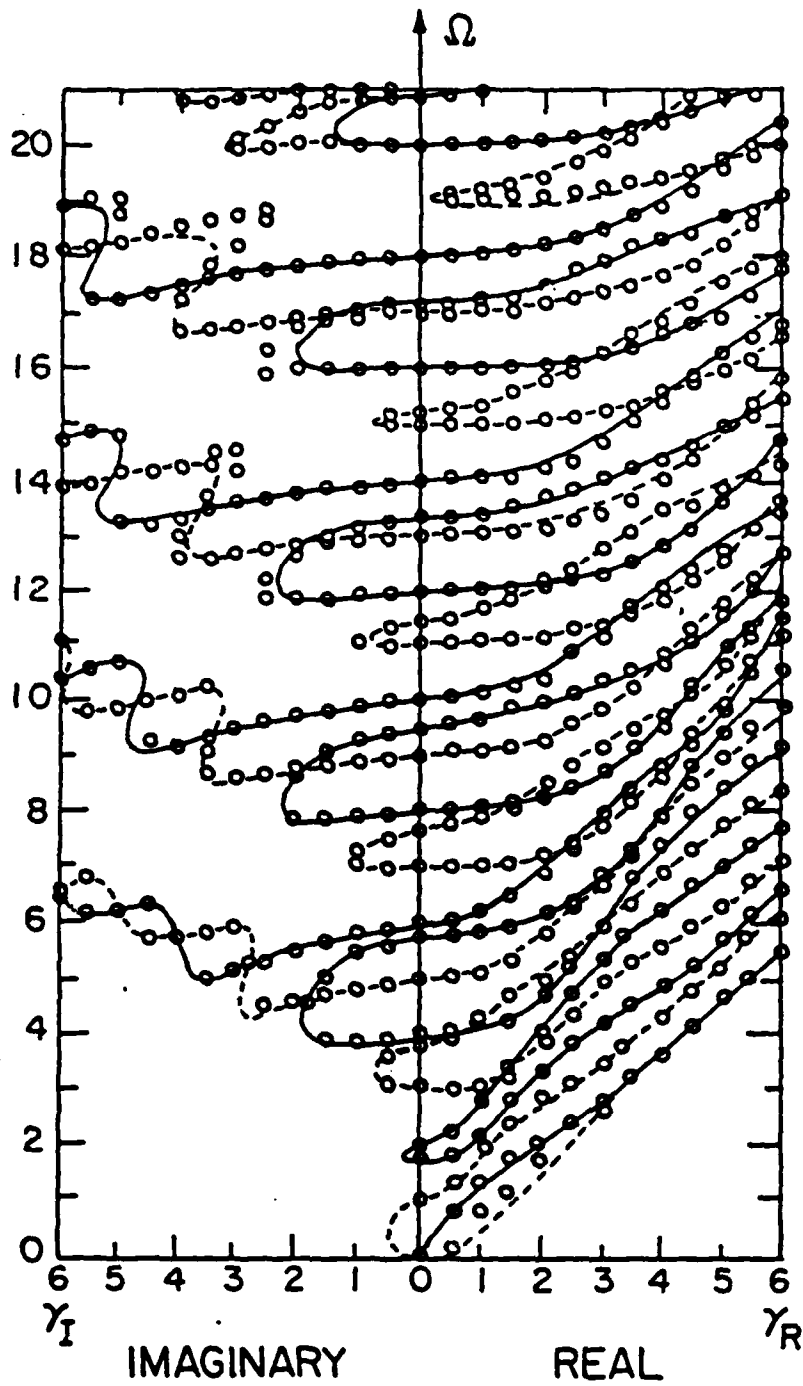


Fig. 2

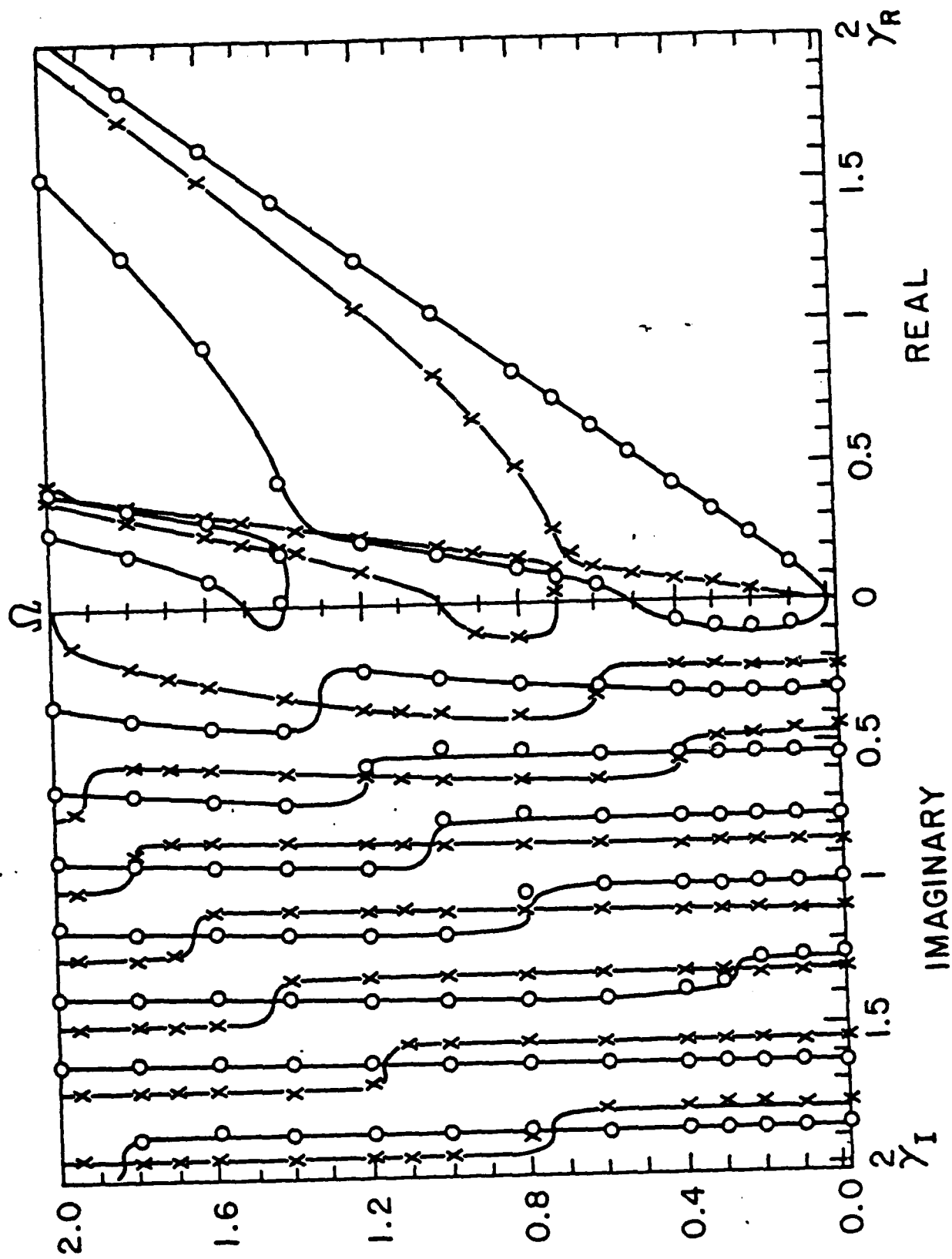


Fig. 4

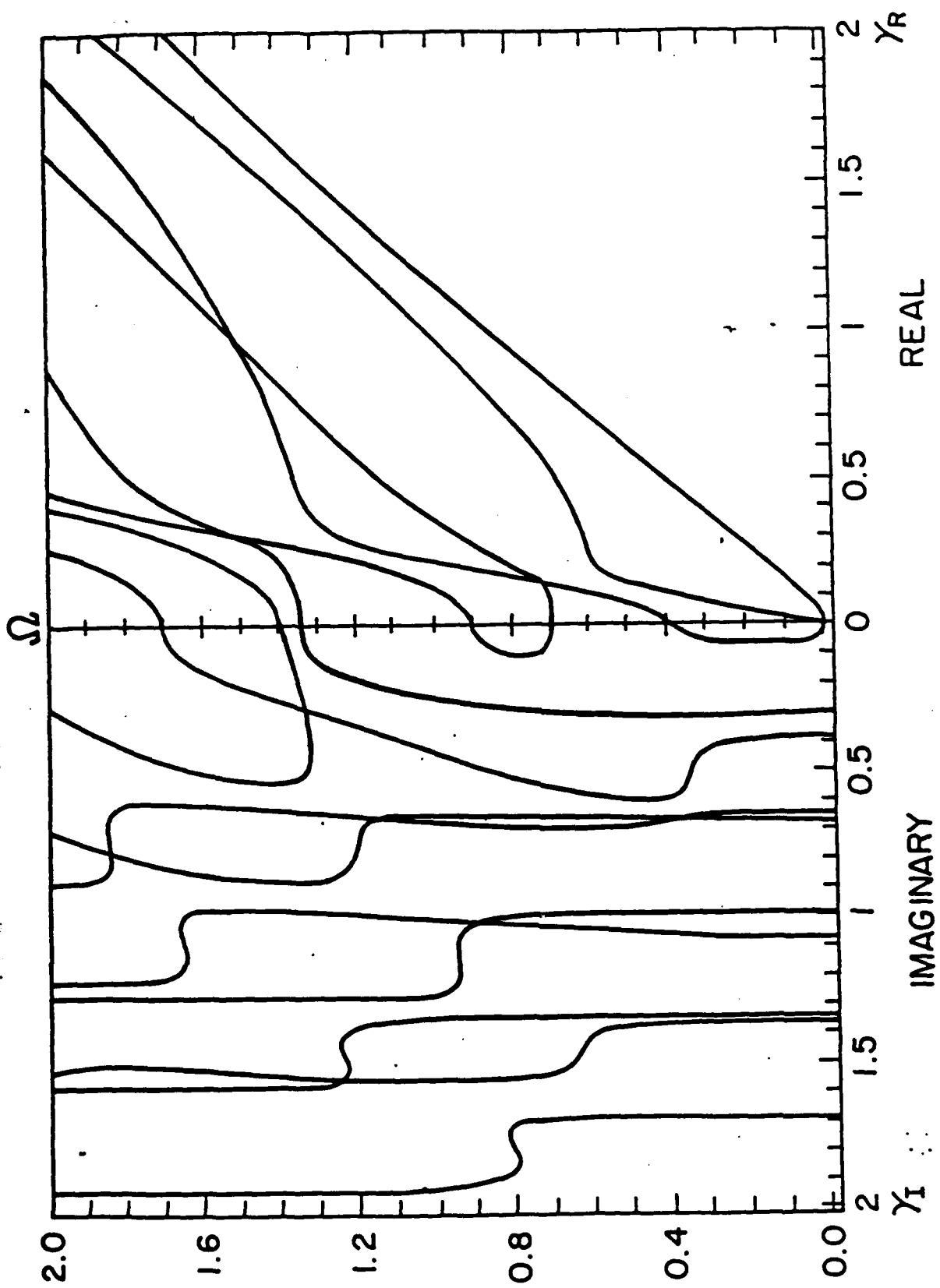


Fig. 5

Contour plot of the order function Ω in the complex plane.

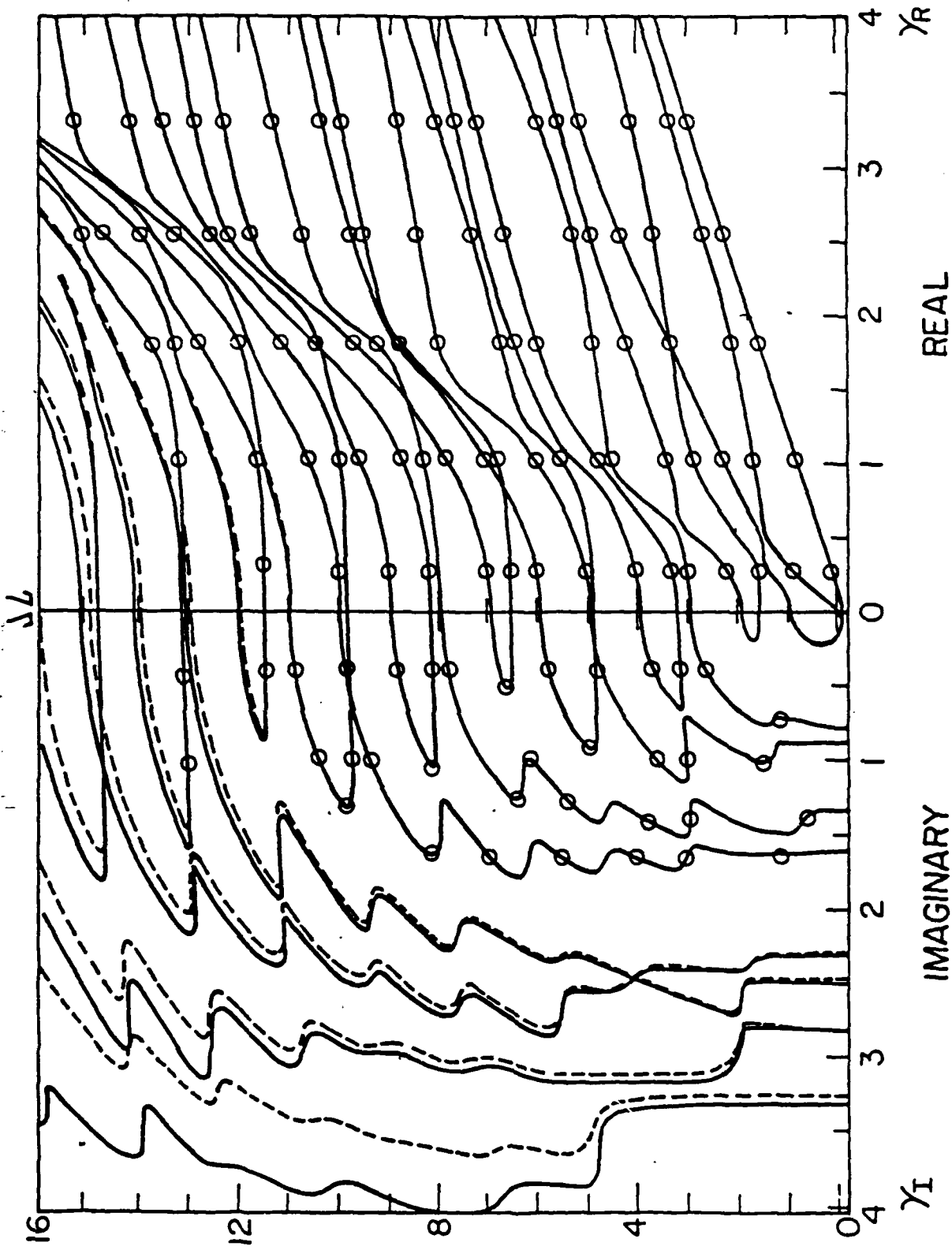


Fig 6

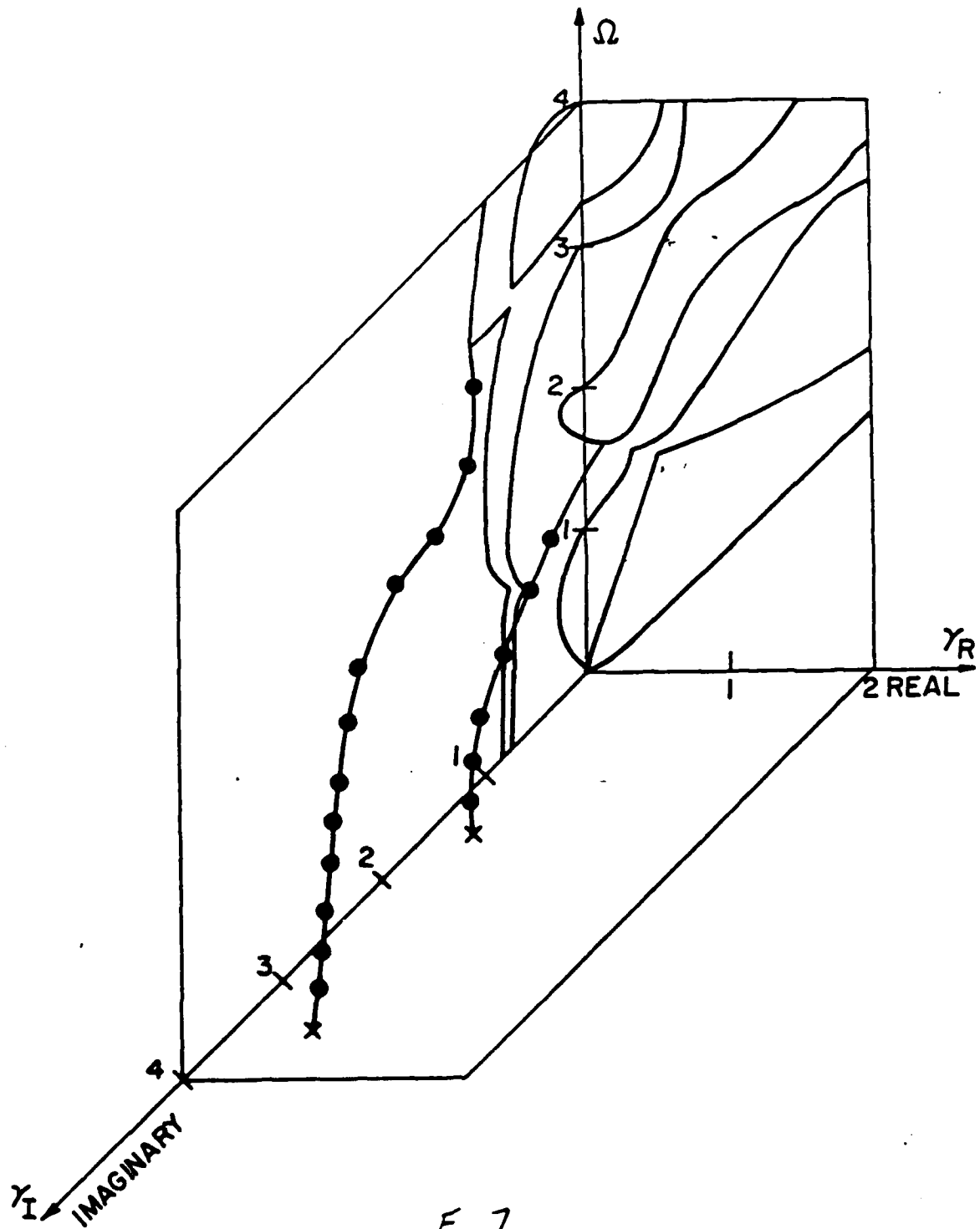


Fig 7

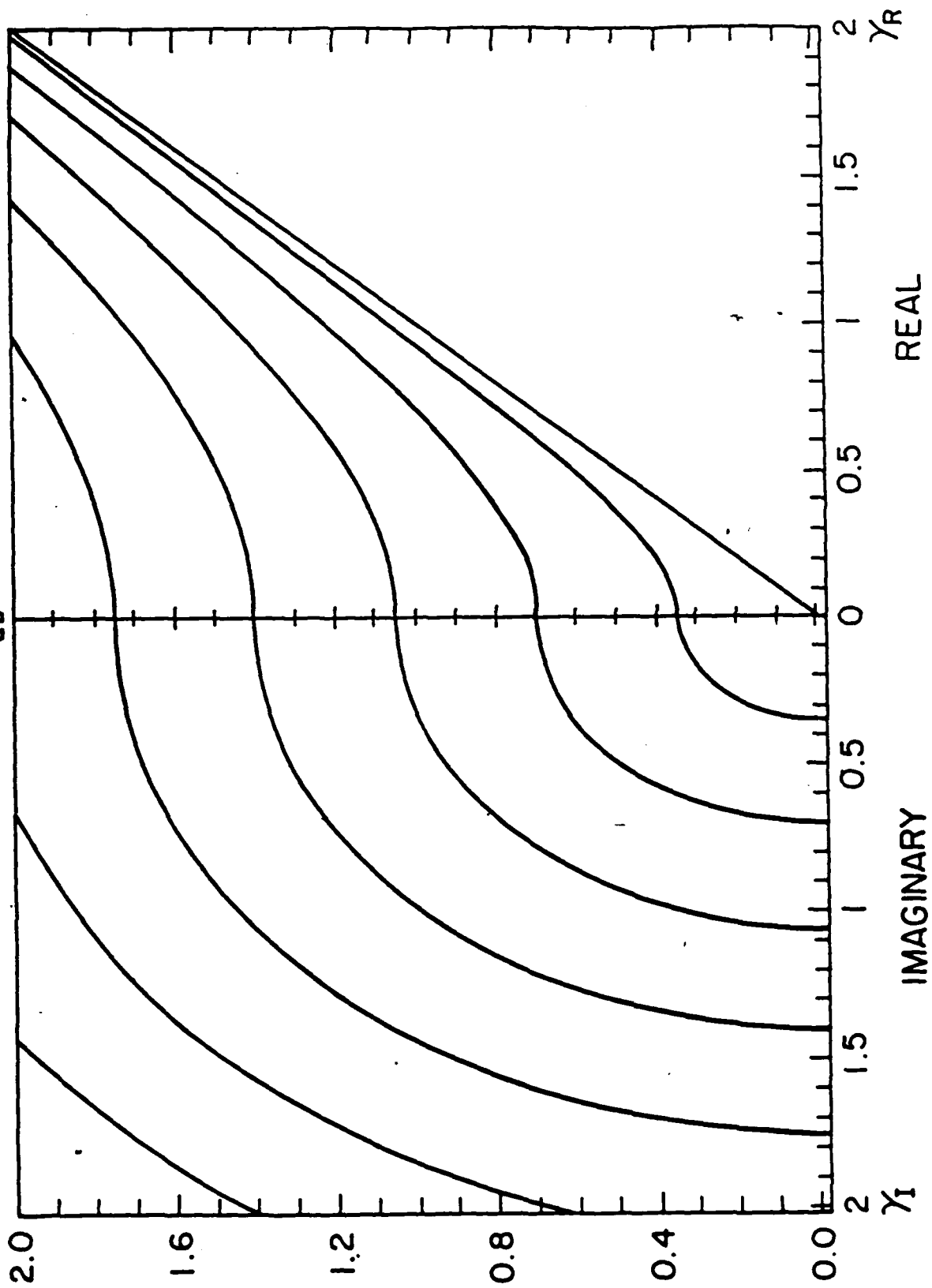


Fig 8

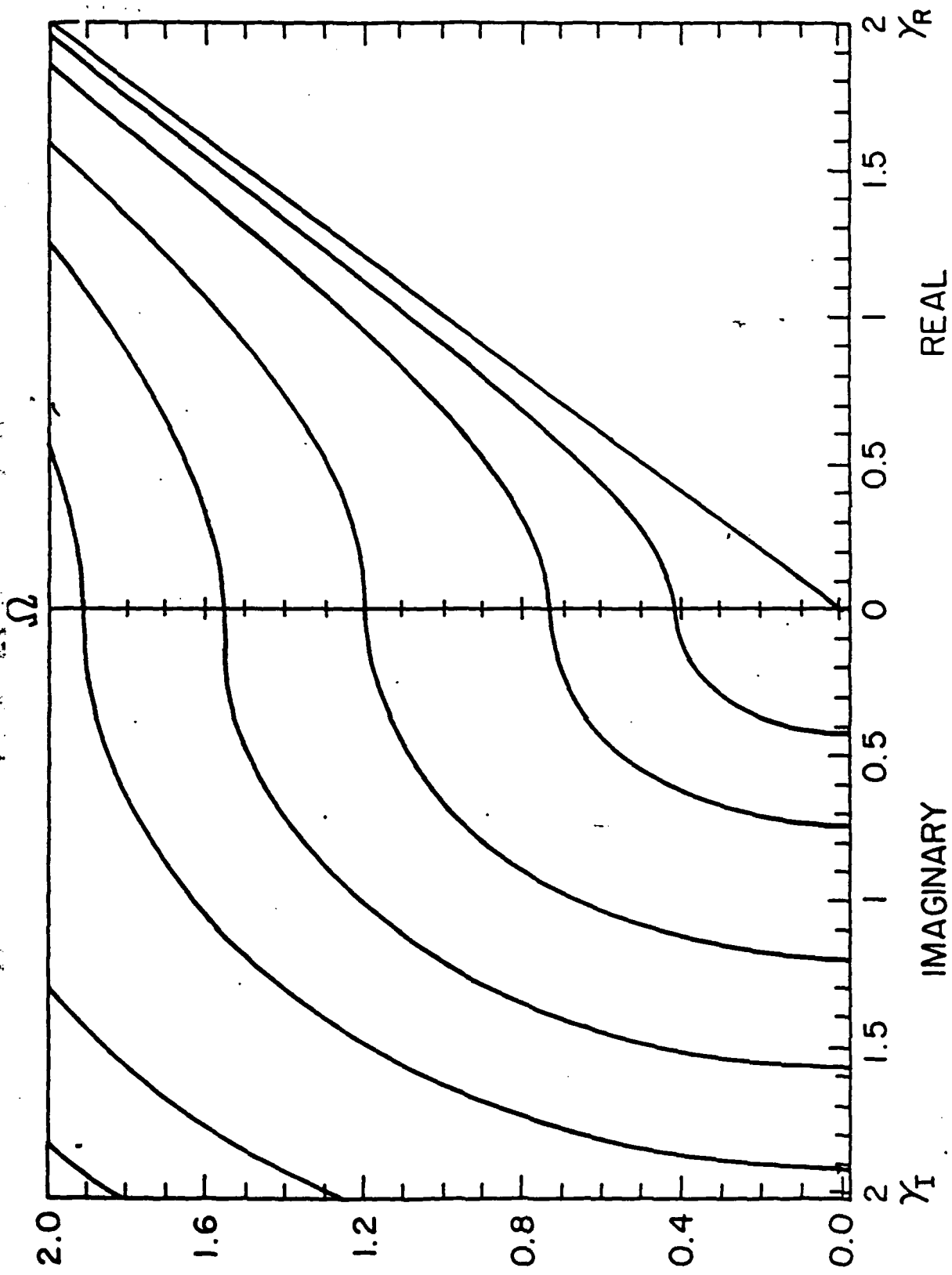


Fig 9

END
DATE
FILMED
5-88
DTIC